

DAWID TALER*, KAROL KACZMARSKI**

A NUMERICAL MODEL OF TRANSIENT PIPELINE OPERATION

NUMERYCZNY MODEL NIEUSTALONEJ PRACY RUROCIĄGU

Abstract

The aim of this study is to develop a numerical model of a steam pipeline. The energy conservation equations for the pipeline wall and steam are solved using the finite volume method (FVM). The transient temperature of the pipeline wall, steam temperature and thermal stresses can be calculated using the model developed in the paper.

Keywords: pipeline heating, transient temperature, numerical model, thermal stresses

Streszczenie

Celem artykułu jest opracowanie modelu numerycznego rurociągu parowego. Równania zachowania energii dla ścianki rurociągu i pary są rozwiązywane przy użyciu metody objętości skończonych (MOS). Nieustalona temperatura ścianki rurociągu, temperatura pary oraz naprężenia cieplne mogą być obliczone za pomocą modelu przedstawionego w artykule.

Słowa kluczowe: nagrzewanie rurociągu, temperatura nieustalona, model numeryczny, naprężenia cieplne

DOI:

* PhD. DSc. Eng. Dawid Taler, Prof. CUT, Institute of Thermal Engineering and Air Protection, Faculty of Environmental Engineering, Cracow University of Technology.

** MSc. Eng. Karol Kaczmariski, Institute of Thermal Power Engineering, Faculty of Mechanical Engineering, Cracow University of Technology.

1. Introduction

High-temperature steam pipelines in steam boilers are used to transport superheated steam from the boiler to the turbine. During start-ups and shutdowns of the power units, as well as during load changes, high thermal stresses can occur in the pipeline wall and in pipeline fittings. Particularly high stresses occur in T-pipes and Y-pipes. Additionally, thick-walled sections with complex shapes such as valves and gate valves are exposed to large thermal loads. Both high thermal stresses and time-variable thermal stresses may lead to the premature damage of pipelines in the form of cracks. Knowledge of the range of stresses in critical components allows conducting the startup of the boiler in a way that provides a safe and long life of the boiler and turbine. Issues relating to the direct and inverse calculation and monitoring of thermal stresses in cylindrical components are the subjects of current research [1, 2]. In this paper, transient temperature and thermal stress distributions in a pipeline connecting the boiler and turbine will be determined. The finite volume method (FVM) is used to determine the transient temperature of the steam and pipeline wall. Thermal stresses are also calculated.

2. Mathematical formulation

A scheme of the pipeline linking the boiler with a turbine in a power unit with a capacity of 120MW is depicted in Fig. 1.

The governing equations for the steam are:

- mass conservation equations

$$\frac{\partial \rho}{\partial t} = -\frac{1}{A} \cdot \frac{\partial \dot{m}}{\partial z} \quad (1)$$

- momentum conservation equations

$$\frac{\partial \dot{m}}{\partial z} = -\frac{\partial}{\partial z} \left(\frac{\dot{m}^2}{\rho \cdot A} \right) - A \cdot \left(\frac{\partial p}{\partial z} + \rho \cdot g \cdot \sin \varphi - \frac{\xi}{d_m} \cdot \frac{|\dot{m}|}{2 \cdot \rho \cdot A^2} \right) \quad (2)$$

- energy conservation equations

$$\rho \cdot c_p \left(\frac{\partial T}{\partial t} + \frac{\dot{m}}{\rho \cdot A} \frac{\partial T}{\partial z} \right) = \beta \cdot T \left(\frac{\partial p}{\partial t} + \frac{\dot{m}}{\rho \cdot A} \frac{\partial p}{\partial z} \right) + \frac{\xi}{d_m} \frac{|\dot{m}^3|}{2 \cdot \rho^2 \cdot A^3} - \frac{\alpha(T - T_w)}{A} + \frac{1}{A} \frac{\partial}{\partial z} \left(A \cdot \lambda \frac{\partial T}{\partial z} \right) \quad (3)$$

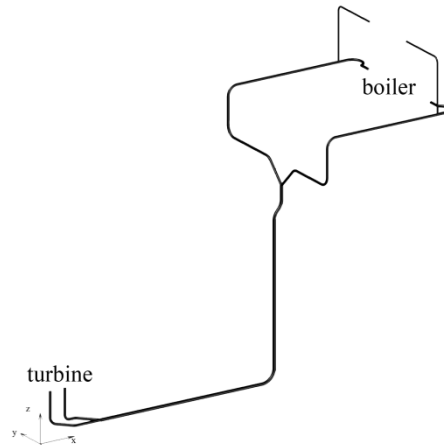


Fig. 1. The pipeline connecting the boiler and turbine

The transient heat conduction equation for the pipeline wall is

$$\rho_w \cdot c_{pw} \frac{\partial T_w}{\partial t} = \nabla \cdot [\lambda_w(T_w) \nabla T_w] \quad (4)$$

The derivative $\partial \rho / \partial t$ in Eq. (1) was assumed to be equal zero since the changes in pressure along the length of the pipeline are small and consequently the steam density can be assumed constant. The assumption $\partial \rho / \partial t = 0$ in Eq. (1) implies that mass flow rate \dot{m} is constant over the tube length, i.e.

$$\dot{m} = \text{const} \quad (5)$$

The velocity of the steam in each cross-section of the pipeline can be calculated from the formula

$$w = \frac{4 \cdot \dot{m}}{\pi \cdot \rho \cdot d_{in}^2} \quad (6)$$

Considering that $\partial \dot{m} / \partial t = 0$, the momentum conservation equation (2) reduces to

$$\frac{d p}{d z} = -\rho \cdot w \frac{d w}{d z} - \rho \cdot g \cdot \sin \varphi - \frac{\xi}{d_{in}} \frac{\rho \cdot w \cdot |w|}{2} \quad (7)$$

Using Eq. (7), the steam pressure can be determined along the path flow.

Neglecting the thermal expansion of the steam ($\beta = 0$), the heat generation due to friction and the axial thermal conduction in the steam, the energy conservation equation (3) for the steam simplifies to the form

$$\rho \cdot c_p \cdot \left(\frac{\partial T}{\partial t} + \frac{\dot{m}}{\rho \cdot A} \cdot \frac{\partial T}{\partial z} \right) = - \frac{\alpha \cdot (T - T_w) \cdot U_{in}}{A} \quad (8)$$

The heat conduction equation (4) in the cylindrical coordinate system is

$$\rho_w \cdot c_{pw} \frac{\partial T_w}{\partial t} = \frac{1}{r} \cdot \frac{\partial}{\partial r} \left[r \cdot \lambda_w(T_w) \frac{\partial T_w}{\partial r} \right] + \frac{\partial}{\partial z} \left[\lambda_w(T_w) \frac{\partial T_w}{\partial z} \right] \quad (9)$$

The system of partial differential equations (8, 9) is subject to the following initial and boundary conditions:

$$T|_{t=0} = T_0 \quad (10)$$

$$T_w|_{t=0} = T_{w,0} \quad (11)$$

$$T|_{x=0} = f(t) \quad (12)$$

$$\lambda_w \frac{\partial T}{\partial r} \Big|_{r=r_{in}} = \alpha(T - T_w) \quad (13)$$

$$\lambda_w \frac{\partial T}{\partial r} \Big|_{r=r_{out}} = 0 \quad (14)$$

$$\lambda_w \frac{\partial T_w}{\partial z} \Big|_{z=0} = 0 \quad (15)$$

$$\lambda_w \frac{\partial T_w}{\partial z} \Big|_{z=L} = 0 \quad (16)$$

In addition to the conditions (10 ÷ 16), the pressure and mass flow rate of the steam are known at the inlet of the pipeline.

The initial-boundary value problem (8 ÷ 16) was solved using the finite volume method (FVM) [3, 4].

First, the computational domain, i.e. the wall and the area occupied by the steam, was divided into finite volumes (Fig. 2).

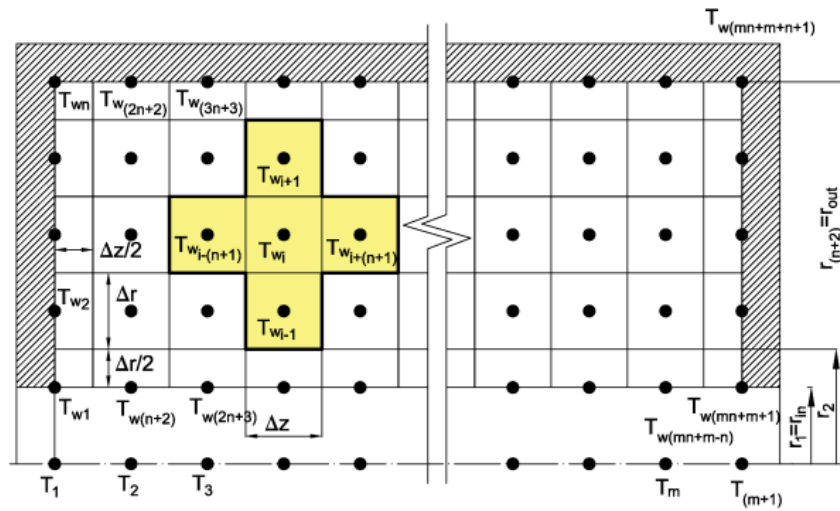


Fig. 2. Division of the computational domain into finite volumes

Energy balance equations were formed for each control volume lying both in the wall and the steam.

For example, the energy balance equation for node i is set for the control volume located in the computational area of the wall (Fig. 3).

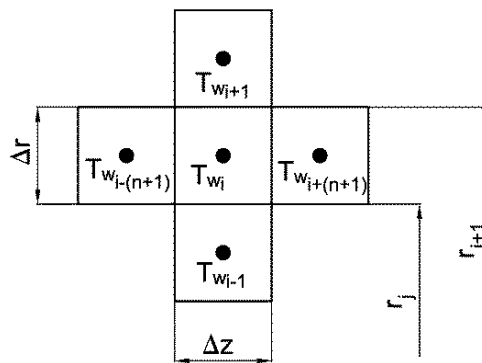


Fig. 3. Wall temperature at the node i and adjacent nodes $i-1, i+1, i-n-1, i+n+1$

The transformation of Eq.(9) gives

$$\frac{dT_{w_i}}{dt} = \frac{a(T_{w_i})}{\lambda_w(T_{w_i})} \left[\frac{r_j}{\Delta r} \frac{\lambda_w(T_{w_i}) + \lambda_w(T_{w_{i-1}})}{r_{j+1}^2 - r_j^2} (T_{w_{i-1}} - T_{w_i}) + \frac{r_{j+1}}{\Delta r} \frac{\lambda_w(T_{w_{i+1}}) + \lambda_w(T_{w_i})}{r_{j+1}^2 - r_j^2} (T_{w_{i+1}} - T_{w_i}) + \frac{\lambda_w(T_{w_{i+n+1}}) + \lambda_w(T_{w_{i-1}})}{2(\Delta z)^2} (T_{w_{i+n+1}} - T_{w_i}) + \frac{\lambda_w(T_{w_{i-n-1}}) + \lambda_w(T_{w_i})}{2(\Delta z)^2} (T_{w_{i-n-1}} - T_{w_i}) \right] \quad (17)$$

In a similar manner, the heat balance equation for the i -th control volume located in the region occupied by steam can be set

$$\frac{dT_{i+1}}{dt} = -\frac{\dot{m}}{\rho(T_i)A} \frac{T_{i+1} - T_i}{\Delta z} - \frac{\alpha(T_i)U_w}{A \cdot \rho(T_i) \cdot c_p(T_i)} \left[\frac{T_{i+1} + T_i}{2} - \frac{T_{w_{i(n+1)-1}} + T_{w_{i(n+1)+1}}}{2} \right] \quad i = 1, \dots, m \quad (18)$$

The heat transfer coefficient α on the inner surface of the pipeline was determined using Gnielinski's correlation [5]

$$Nu = \frac{(\xi/8) \cdot (Re - 1000) \cdot Pr}{1 + 12.7 \cdot (\xi/8)^{1/2} \cdot (Pr^{2/3} - 1)} \left[1 + \left(\frac{d_{in}}{L} \right)^{2/3} \right] \quad (19)$$

where the friction factor ξ is given by the Colebrook correlation

$$\xi = [1.8 \cdot \log(Re) - 1.51]^{-2} \quad (20)$$

The Reynolds number, Prandtl number, and Nusselt number are defined as

$$Re = \frac{\rho \cdot w \cdot d_{in}}{\mu}, \quad Pr = \frac{c_p \cdot \mu}{\lambda}, \quad Nu = \frac{\alpha \cdot d_{in}}{\lambda} \quad (21)$$

After the formulation of all balance equations for the wall and steam, a system of ordinary differential equations for node temperatures is obtained. The number of equations for the nodes lying in the wall area is $(m + 1)(n + 1)$, while for the steam, it is $(m + 1)$.

The system of ordinary differential equations was solved by the Runge-Kutta method of the fourth order.

To ensure the stability of determining the wall and steam temperature the Fourier stability condition for the wall and Courant-Friedrichs-Levy condition for the steam should be satisfied. The smallest allowable time step Δt_{max} results from the Courant-Friedrichs-Levy condition [6]

$$\frac{w_i \cdot \Delta t}{\Delta z} \leq 1, \quad i = 1, \dots, m + 1 \quad (22)$$

Thermal stresses can be determined after calculating the transient temperature distribution in the wall.

Considering that the axial component of the temperature gradient $\partial T_w/\partial z$ is very small, only the radial temperature drop in the wall of the pipeline is taken into account. Assuming that the ends of the pipeline are free to lengthen, the thermal stress components are given by the following formulas [7]:

$$\sigma_r = \frac{E \cdot \beta_T}{2 \cdot (1-\nu)} \cdot \left(1 - \frac{r_{in}^2}{r^2}\right) \cdot [\bar{T}(t) - \bar{T}(r,t)] \quad (23)$$

$$\sigma_\varphi = \frac{E \cdot \beta_T}{2 \cdot (1-\nu)} \cdot \left[\left(1 - \frac{r_{in}^2}{r_2^2}\right) \cdot \bar{T}(t) + \left(1 - \frac{r_{in}^2}{r_2^2}\right) \cdot \bar{T}(r,t) - 2 \cdot T(r,t) \right] \quad (24)$$

$$\sigma_z = \frac{E \cdot \beta_T}{1-\nu} \cdot [\bar{T}(t) - T(r,t)] \quad (25)$$

where the mean wall temperature $T(t)$

$$\bar{T}(t) = \frac{2}{r_{out}^2 - r_{in}^2} \int_{r_{in}}^{r_{out}} r \cdot T \, dr \approx \frac{2 \cdot \Delta r}{r_{out}^2 - r_{in}^2} \left[r_2 \frac{T_1 + T_2}{2} + r_{n+1} \frac{T_n + T_{n+1}}{2} + \sum_{i=2}^{n-1} \frac{r_i + r_{i+1}}{2} T_i \right] \quad (26)$$

$$\bar{T}(r,t) = \bar{T}(r_i,t) = \frac{2}{r^2 - r_{in}^2} \int_{r_{in}}^r r \cdot T \, dr \approx \frac{2 \cdot \Delta r}{r_i^2 - r_{in}^2} \left[r_2 \frac{T_1 + T_2}{2} + \sum_{j=2}^i \frac{r_j + r_{j+1}}{2} T_j \right] \quad (27)$$

where

$$\begin{aligned} r_2 &= r_1 + \frac{\Delta r}{2} \\ r_i &= r_2 + (i-2) \cdot \Delta r, \quad i = 3, \dots, n+1 \\ r_{n+2} &= r_{n+1} + \frac{\Delta r}{2} \end{aligned} \quad (28)$$

Radial stresses σ_r are equal to zero on the inner and outer pipeline surfaces – circumferential σ_φ and axial stresses σ_z are equal on these surfaces.

3. Results

The paper presents the results of calculations concerning the pipeline connecting the boiler OP-380 with a steam turbine.

The steam pipeline is made of low-alloy steel 13HMF (C-0.18%, Mn-0.40%, Si-0.35%, P_{max}-0.040%, S_{max}-0.040%, Cu_{max}-0.25%, Cr-0.60%, Ni_{max}-0.30%, Mo-0.65%, Al_{max}-0.020%). The main dimensions are: outer diameter $d_{out} = 0.324$ m, wall thickness

$b = 0.04$ m, and length $L = 45$ m. The physical properties of steel are a function temperature:

$$\lambda = 48.495 + 0.0012 \cdot T - 6.46 \cdot 10^{-5} \cdot T^2 + 4.175 \cdot 10^{-8} \cdot T^3 \quad (29)$$

$$a = 1.341 \cdot 10^{-5} - 3.452 \cdot 10^{-9} \cdot T - 3.193 \cdot 10^{-11} \cdot T^2 + 2.853 \cdot 10^{-14} \cdot T^3 \quad (30)$$

where the thermal conductivity λ is in W/(m·K), the thermal diffusivity a is in m²/s, and the temperature T is in °C.

The temperature of the wall in the radial direction is computed in five evenly-spaced nodes ($n = 4$). The number of nodes in the axial direction is $m + 1 = 21$. The calculation of the transient temperature of the fluid and pipeline wall was carried out for a different number of finite volumes across the thickness of pipe wall.

Inspection of the results shown in Fig. 4 illustrates that even at four finite volumes, i.e. for the five nodes evenly distributed over the wall thickness, satisfactory accuracy of the calculations is obtained.

Almost identical results are obtained for the division of the pipe wall into nine (10 nodes) or nineteen finite volumes (20 nodes) as were obtained for the division into four finite volumes (5 nodes) Fig. 4.

The temperature of the wall in the radial direction is computed in five evenly-spaced nodes ($n = 4$). The number of nodes in the axial direction is $m + 1 = 21$.

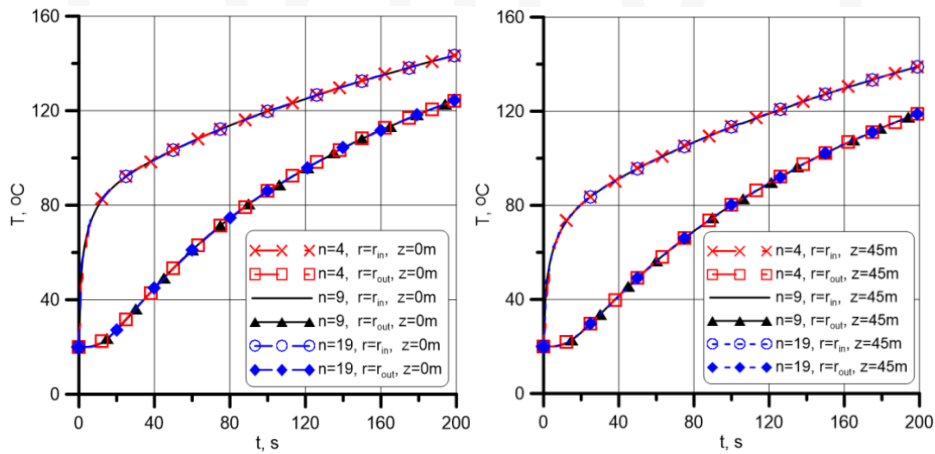


Fig. 4. The temperature of the inner and outer surface of the pipeline at the inlet $z = 0$ m (a) and outlet $z = 45$ m (b), as a function of time t for various numbers of control volumes n across the thickness of the pipeline wall

The pressure is $p = 13.9$ MPa. The mass flow rate of the steam is $\dot{m} = 105.55$ kg/s. The initial temperature of the pipeline and steam is $T_{w0} = 20^\circ\text{C}$. At time $t > 0$, the temperature of the steam pipeline inlet increases abruptly to a constant temperature of $T_0 = 540^\circ\text{C}$.

Selected modelling results are shown in Figures 5 ÷ 9. The steam temperature as a function of time at nodes no. 2 ($z = 2.25$ m), no.10 ($z = 20.25$ m), and no. 20 ($z = 42.75$ m) are displayed in Fig. 5.

The analysis of the results shown in Fig. 5 shows that after about 600 seconds, steam temperature reaches a steady state.

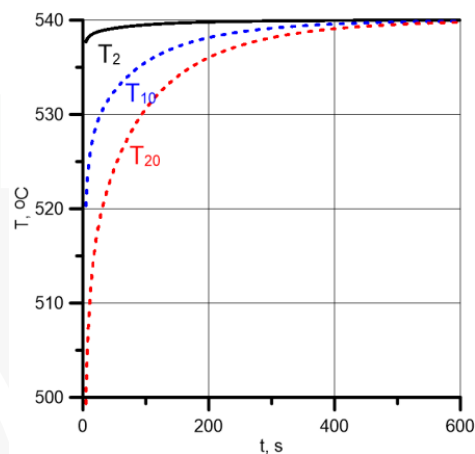


Fig. 5. Steam temperature as a function of time at nodes no. 2 ($z = 2.25$ m), no. 10 ($z = 20.25$ m) and no. 20 ($z = 42.75$ m)

Fig. 6 illustrates steam temperature changes over the length of the pipeline at time points 10s, 60s, 240s, and 600s.

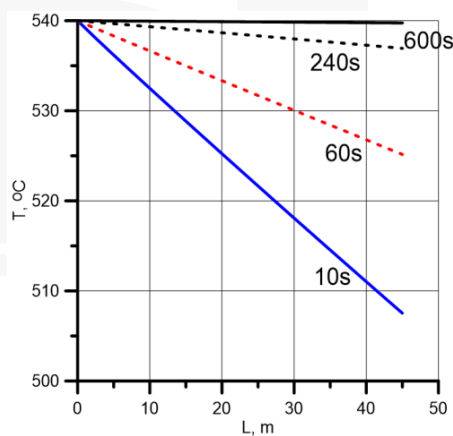


Fig. 6. Steam temperature changes over the length of the pipeline at time points 10 s , 60 s, 240 s, and 600 s

Fig. 7 depicts the pipeline wall temperature in two different cross-sections as a function of time. The wall temperature is shown in five uniformly spaced nodes. Nodes 11 and 101

are located on the inner surface while nodes 15 and 105 lie on the outer surface of the pipeline.

At the beginning of the heating process, the temperature differences over the thickness of the wall are large but rapidly decrease over time (Fig. 7).

Circumferential stresses on the inner and outer surface of the pipeline as a function of time are presented in Fig. 8.

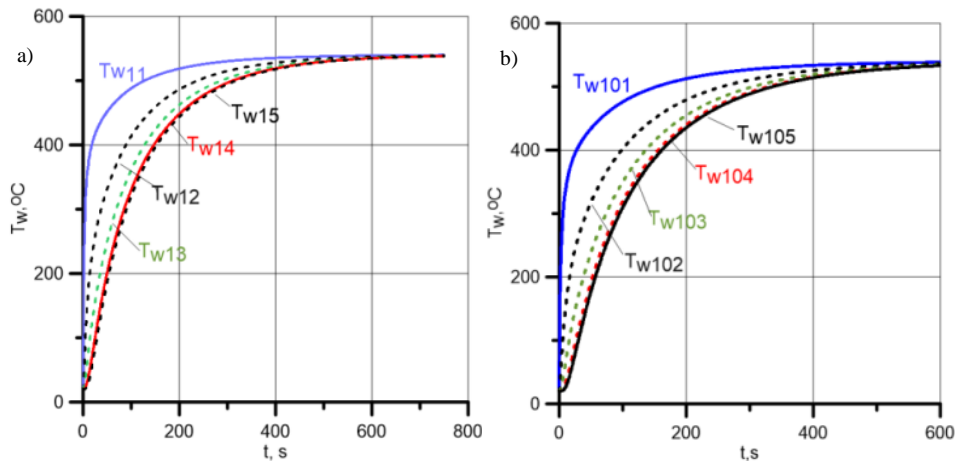


Fig. 7. Wall temperature in tree cross-sections as a function of time a) $z = 2.25$ m, b) $z = 42.75$ m

The analysis of the results presented in Fig. 8 shows that the inner surface is exposed to high compressive stresses while on the outer surface, substantially lower tensile stresses occur.

High thermal stresses in the pipeline are caused by a high jump of 520 K in steam temperature at time $t = 0$.

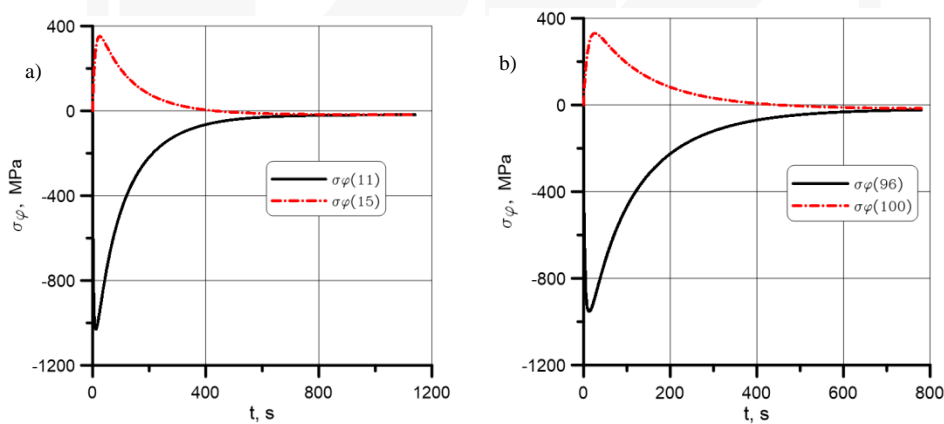


Fig. 8. Circumferential thermal stress on the inner (nodes 11 and 96) and outer (nodes 15 and 100) surfaces of the pipeline as a function of time; a) $z = 2.25$ m, b) $z = 42.75$ m

The largest absolute value of stress occurs at the beginning of heating and tends to zero over time Fig. 8.

4. Summary

The mathematical model of the steam pipeline heating developed in the paper allows determining the temperature of the steam and the pipeline wall as a function of position and time. It is possible to determine transient thermal stresses caused by the temperature difference across the wall thickness using the developed model. Examples of calculations of the steam temperature, wall temperature and circumferential thermal stresses on the inner and outer surface of the pipeline have been presented. The calculation tests performed in the paper show that the developed mathematical model can be used to simulate the actual pipeline heating or cooling in a power plant.

Nomenclature

a	– thermal diffusivity $a = \lambda/(c \rho)$, m^2/s
b	– wall thickness, m
A	– cross-section area, m^2
c_p	– specific heat capacity, $\text{J}/(\text{kg}\cdot\text{K})$
d_{in}	– inner diameter, m
d_{out}	– outer diameter, m
E	– modulus of elasticity (Young's modulus), Pa
f	– fluid temperature at the inlet of the pipeline, $^{\circ}\text{C}$
g	– gravity acceleration, m/s^2
L	– length of the pipeline, m
$(m+1)$	– number of nodes in the longitudinal direction
\dot{m}	– fluid mass flow rate, kg/s
$(n+1)$	– number of nodes in radial direction
Nu	– Nusselt number
p	– absolute pressure, Pa
Pr	– Prandtl number
r	– radius, m
r_{in}	– inner radius, m
r_{out}	– outer radius, m
Re	– Reynolds number
T	– temperature, $^{\circ}\text{C}$ or K
t	– time, s
$\bar{T}(t)$	– mean temperature on the wall thickness, $^{\circ}\text{C}$ or K
$\bar{T}(r, t)$	– mean temperature of the wall between r_{in} and r , $^{\circ}\text{C}$ or K
U_{in}	– inner perimeter of the tube, m
w	– fluid velocity, m/s

Greek symbols

α	– heat transfer coefficient, $W/(m^2 \cdot K)$
β	– volumetric thermal expansion coefficient, $1/K$
β_T	– linear thermal expansion coefficient, $1/K$
Δr	– radial step, m
Δt	– time step, s
Δz	– axial step, m
λ	– thermal conductivity, $W/(m \cdot K)$
μ	– dynamic viscosity, $Pa \cdot s$
ν	– Poisson's ration
ξ	– friction fraction
ρ	– density, kg/m^3
σ_r	– radial stress component, Pa
σ_φ	– circumferential stress component, Pa
σ_z	– axial stress component, Pa
φ	– inclination angle of the pipeline with respect to the horizontal plane

Subscripts

i	– node number
in	– inner surface
out	– outer surface
w	– wall

References

- [1] Taler J., Zima W, Jaremkiewicz M., *Simple method for monitoring transient thermal stresses in pipelines*, Journal of Thermal Stresses, 39(4), 2016, 386-397.
- [2] Dzierwa P., Taler D., Taler J., *Optimum heating of cylindrical pressure vessels*, Forsch Ingenieurwes, 80, 2016, DOI 10.1007/s10010-016-0196-7.
- [3] Taler J., Duda P., *Solving Direct and Inverse Heat Conduction Problems*, Springer, Berlin-Heidelberg 2006.
- [4] Taler D., *Dynamics of tube heat exchangers*, Dissertation and monographs 193, Publishing House of AGH, Cracow 2009.
- [5] Gnieliński V., *New Equation for Heat and Mass Transfer in Turbulent Pipe and channel flow*, Int. Chem. Engng. 16, 1976, 359-368.
- [6] Pletcher R.H., Tannehill J.C., Anderson D., *Computational Fluid Mechanics and Heat Transfer*, Third edition, CRC Press, Boca Raton 2013.
- [8] Hetnarski R.B., Noda N. Tanigawa Y., *Thermal Stresses*, Second Edition Solution Manual, Taylor & Francis Inc, Boca Raton 2002.